Stromal epigenetic dysregulation is sufficient to initiate mouse prostate cancer via paracrine Wnt signaling

Yang Zong[a], Jiaoti Huang[b], Devipriya Sankarasharma[c], Teppei Morikawa[d], Masashi Fukayama[d], Jonathan I. Epstein[e], Kiran K. Chada[c], and Owen N. Witte[a,f,g,h,1]

[a]Howard Hughes Medical Institute, University of California, Los Angeles, CA 90095; [b]Department of Pathology and Laboratory Medicine, [f]Eli and Edythe Broad Center of Regenerative Medicine and Stem Cell Research, [g]Department of Microbiology, Immunology, and Molecular Genetics, and [h]Department of Molecular and Medical Pharmacology, David Geffen School of Medicine, University of California, Los Angeles, CA 90095; [c]Department of Biochemistry, University of Medicine and Dentistry of New Jersey–Robert Wood Johnson Medical School, Piscataway, NJ 08554; [d]Department of Pathology, Graduate School of Medicine, University of Tokyo, Tokyo 113-0033, Japan; and [e]Departments of Pathology, Urology, and Oncology, The Johns Hopkins Hospital, Baltimore, MD 21231

Contributed by Owen N. Witte, October 24, 2012 (sent for review September 19, 2012)

Carcinomas most often result from the stepwise acquisition of genetic alterations within the epithelial compartment. The surrounding stroma can also play an important role in cancer initiation and progression. Given the rare frequencies of genetic events identified in cancer-associated stroma, it is likely that epigenetic changes in the tumor microenvironment could contribute to its tumor-promoting activity. We use Hmga2 (High-mobility group AT-hook 2) an epigenetic regulator, to modify prostate stromal cells, and demonstrate that perturbation of the microenvironment by stromal-specific overexpression of this chromatin remodeling protein alone is sufficient to induce dramatic hyperplasia and multifocal prostatic intraepithelial neoplasia lesions from adjacent naïve epithelial cells. Importantly, we find that this effect is predominantly mediated by increased Wnt/β-catenin signaling. Enhancement of Hmga2-induced paracrine signaling by overexpression of androgen receptor in the stroma drives frank murine prostate adenocarcinoma in the adjacent epithelial tissues. Our findings provide compelling evidence for the critical contribution of epigenetic changes in stromal cells to multifocal tumorigenesis.

Prostate cancer is the leading nondermatologic malignancy for males in many developed countries (1). Primary prostate cancer often presents as a multifocal malignant disorder, consisting of multiple disparate tumor clones with distinct histological features and heterogeneous biological behaviors (2). The interfocal heterogeneity is generally believed to be caused by genetic or epigenetic alterations occurring synchronously or metachronously in the epithelia during cancer evolution. However, an aberrant tumor microenvironment may provide "field effects" (3) to facilitate the development of multiclonal neoplastic lesions.

Increasing evidence demonstrates that genetic alterations in individual constituents of the mesenchyme can disrupt epithelial homeostasis, triggering tumor formation from neighboring epithelial cells (4, 5). Targeted inactivation of TGF-beta receptor type-2 in mouse fibroblasts led to prostatic intraepithelial neoplasia (PIN) and squamous cell carcinoma of the forestomach (4). Previous work from our laboratory has shown that enhanced mesenchymal expression of FGF10 induces the formation of PIN or prostate adenocarcinoma (5). Van Dyke's group showed that cancer cells impose selective pressure on the surrounding stroma, which stimulates the clonal expansion of cancer-associated fibroblasts (CAFs) and in turn promotes tumor progression (6). Moreover, cancer cells can influence their microenvironment by recruiting bone marrow-derived inflammatory cells and inducing profound changes in the extracellular matrix (ECM), which fuels tumor survival, growth, invasion, and metastasis (7).

Reciprocal communication between cancer cells and their microenvironment is evident during tumor evolution; however, the mechanisms for the phenotypic and molecular changes in CAFs remain uncertain. Despite certain genetic alterations found in stromal cells from various cancers (8), the absence of detectable genetic changes has been described in CAFs from breast and ovarian carcinomas, accompanied by dramatic changes in expression of genes encoding secreted or cell surface proteins (9, 10). Despite their tumor-promoting function, it has been reported that CAFs generally lack cell-intrinsic oncogenic properties (11). These findings raise the possibility that epigenetic changes including DNA methylation, histone modifications, and chromatin remodeling may contribute to the tumor-promoting trait of CAFs. Using methylation-specific digital karyotyping, Hu et al. (12) showed that numerous genomic loci were differentially methylated in the stroma from normal breast tissue and breast carcinomas, suggesting that altered DNA methylation may be one mechanism for phenotypic and molecular changes in CAFs. However, little is known regarding how stromal epigenetic alterations occur during tumor–mesenchymal interactions. More importantly, the functional consequences of these epigenetic changes in the mesenchyme on tumorigenesis remain unclear.

Given the biological similarities between embryonic development and cancer progression, it is postulated that several pathways involved in the epithelial–mesenchymal interactions during prostate development could be inappropriately reactivated during tumorigenesis (13). Recent studies of gene expression profiles

Significance

Increasing evidence supports the notion that an aberrant microenvironment facilitates cancer development. The mechanisms underlying the phenotypic changes and the tumor-promoting function of cancer-associated stroma remain largely unknown. Overexpression of the chromatin remodeling protein Hmga2 in the stroma leads to the formation of multifocal prostatic precancerous lesions in the neighboring naïve epithelium in a paracrine Wnt-dependent manner. The potent growth-promoting effects of Hmga2-modified stroma collaborate significantly with enhanced stromal AR signaling to drive the development of prostate adenocarcinoma. Our findings provide compelling evidence for the critical contribution of epigenetic changes in stromal cells to cancer initiation and progression.

Author contributions: Y.Z. and O.N.W. designed research; Y.Z. performed research; D.S., T.M., M.F., J.I.E., and K.K.C. contributed new reagents/analytic tools; Y.Z., J.H., D.S., K.K.C., and O.N.W. analyzed data; and Y.Z. and O.N.W. wrote the paper.

The authors declare no conflict of interest.

Freely available online through the PNAS open access option.

[1]To whom correspondence should be addressed. E-mail: owenwitte@mednet.ucla.edu.

This article contains supporting information online at www.pnas.org/lookup/suppl/doi:10.1073/pnas.1217982109/-/DCSupplemental.

in embryonic stem cells (ESCs), adult stem cells, and various human cancers reveal that the ESC-like gene signature is activated in diverse epithelial cancers including prostate cancer and is associated with poor differentiation status and an unfavorable outcome (14, 15). However, because most of these microarray data were generated from bulk tumor tissues, it is unclear whether the activated ESC-like program is expressed in cancer stem cells, the entire malignant epithelia, or in the surrounding stroma. It remains unknown how these embryonic regulatory networks reawaken during cancer evolution. In light of the recent findings about reprogramming of adult fibroblasts to pluripotency with defined factors (16, 17) and the intriguing contribution of epigenetic remodeling to reprogramming efficiency (18), we hypothesized that epigenetic modifications in the stromal cells that reverse their chromatin status and growth-promoting potential toward the embryonic state could be one of the mechanisms for activation of the ESC-like program in cancers. In this study, we chose Hmga2 (High-mobility group AT-hook 2), a downstream target of Lin28 (19), to test this hypothesis.

Hmga2 is a member of the high mobility group family of nonhistone chromatin remodeling proteins implicated in embryonic development, tumorigenesis, and self-renewal of stem cells (20, 21). By binding to AT-rich DNA and interacting with histone-modifying enzymes and other proteins in enhanceosomes and chromatin, Hmga2 functions as a global epigenetic regulator (22, 23). Using a dissociated prostate regeneration approach (24), we examined the contribution of Hmga2-modified stroma to prostate cancer initiation and progression and found that overexpression of stromal Hmga2 was extraordinarily potent and led to the development of multifocal PIN in a paracrine Wnt-dependent manner. Enhancement of Hmga2-induced paracrine signaling by elevated expression of androgen receptor (AR) in the stroma resulted in frank carcinoma in the adjacent epithelial tissues, suggesting that changes in the microenvironment are sufficient to drive epithelial cancer progression.

Results

Hmga2 Expression in Developing Urogenital Sinus and Adult Murine Prostate. Hmga2 is highly expressed throughout the whole early embryo, subsequently restricted to mesenchymal derivatives, and becomes undetectable in most adult tissues (25). Using in situ hybridization, Hmga2 expression was mainly observed in the mesenchyme of the developing mouse lung (26). In murine embryonic [embryonic day (E) 16] urogenital sinus (UGS) that gives rise to the prostate, Hmga2 protein was expressed at higher levels in the stroma relative to p63-positive epithelial cells (Fig. 1*A*). In the cultured UGS mesenchymal (UGSM) cells that were originally derived from E16 mouse UGS mesenchyme, significant levels of Hmga2 can be detected by quantitative RT-PCR (Fig. 1*B*). Immunoblotting analysis of UGSM cells with an antibody against Hmga2 revealed two dominant bands, with the gradual diminution of the upper band during in vitro passage of UGSM cells (Fig. 1*C*). The shift in immunoblotting band patterns may reflect changes in posttranslational modification of Hmga2, such as phosphorylation (27) during cell culture. The mesenchymal-specific expression patterns of Hmga2 in the developing prostate and lung indicate that Hmga2 may play pivotal roles in controlling chromatin status in embryonic mesenchyme during organogenesis.

In addition to high expression in many embryonic tissues, low levels of Hmga2 have been reported in testis, skeletal muscle, and white adipose tissue of adult mice (28). Our previous study showed that prostatic stromal cells can be enriched from adult mouse prostate by flow cytometry using Lin-CD49f-Sca-1$^+$ markers (29). We examined endogenous Hmga2 expression in adult murine prostate and found that relative to prostate epithelial cells, significant levels of Hmga2 could be detected by real-time RT-PCR and immunohistochemistry (IHC) staining in the adult stroma (Fig. S1 *A* and *B*), but the expression levels are much lower compared with those in UGSM cells (Fig. 1*B*). Surgical castration induced up-regulation of Hmga2 mRNA expression in Lin-CD49f-Sca-1$^+$ prostatic stromal cells from adult mice, which could be reversed by androgen resupplementation (Fig. S1 *C* and *D*). These findings are consistent with previous studies (30), suggesting that Hmga2 expression is retained in certain mesenchymal cells in several adult tissues and can be significantly induced by stress conditions.

Prostate development is a dynamic process, which is precisely orchestrated by epithelial–mesenchymal interactions in concert with systemic hormones. The mesenchymal-specific expression of Hmga2 in the mouse prostate prompted us to test the biological function of Hmga2 in prostate development and tumorigenesis. We examined prostates from *Hmga2* knockout mice (25) at 11–14 wk of age and observed a remarkably smaller prostate phenotype compared with the age-matched wild-type controls (Fig. 1*D*), which is disproportionate to the 60% reduction in body size and 40–50% reduction in most organ weights (21, 25). All of the lobes of *Hmga2* null prostates exhibited a blunted appearance, with significantly diminished branching. There was more than a sixfold decrease in cell number from *Hmga2* null prostates, relative to the age-matched wild-type controls (Fig. 1*E*). The histological analysis of *Hmga2* null prostates revealed an apparent diminution in the number of tubules throughout all lobes, associated with a significant loss of secretions, particularly in the anterior lobes (Fig. 1*F*). There was no significant difference in cell proliferative index between wild-type and *Hmga2* null prostates, assessed by proliferating cell nuclear antigen (PCNA) staining. These findings suggest that Hmga2 may play an important role in ductal morphogenesis and regulation of epithelial differentiation during prostate development.

Hmga2-Modified Stroma Induces Hormone-Sensitive Murine PIN Lesions. To test the consequences of Hmga2 overexpression in prostate stromal cells, a lentiviral vector containing the mouse *Hmga2* complete coding sequence and red fluorescent protein (*RFP*) was used to stably overexpress Hmga2 in UGSM cells (Fig. 2*B*). The modified UGSM cells were combined with dissociated adult prostate cells from wild-type mice and subsequently engrafted into the subrenal capsules of male host mice (Fig. 2*A*). Strikingly, the grafts with Hmga2-modified stroma weighed approximately 80 times as much as the control grafts with RFP-expressing stroma at 10 wk after engraftment (Fig. 2*C*).

Histological examination revealed the development of preneoplastic lesions in Hmga2-UGSM grafts, with progressive epithelial proliferation and hyperplasia in a cribriform pattern accompanied by nuclear atypia and remarkably dilated lumens containing abundant secretions (Fig. 2*D*). Other than pronounced tubular enlargement, the histology of Hmga2-UGSM grafts was indistinguishable from high-grade PIN, which was previously reported in mouse models with prostate epithelial-specific oncogene expression or tumor suppressor inactivation (31–33). IHC analysis with an anti-PCNA antibody showed significant increase in the percentage of PCNA$^+$ cells in PIN lesions (Fig. S2). Both the RFP fluorescent signal and anti-Hmga2 staining were restricted to the thin fibromuscular layer surrounding PIN lesions induced by Hmga2-modified stroma (Fig. 2*E*), and no significant outgrowth of stromal cells was observed in tissue recombinants consisting of Hmga2-USGM cells. These findings suggest that Hmga2 overexpression in UGSM cells did not transform the mesenchymal cells but led to a precancerous phenotype from adjacent naïve epithelial cells. In addition, the epithelial identity in preneoplastic lesions was further confirmed by utilization of adult prostate cells from GFP transgenic mice (Fig. 3*A*) as well as staining with epithelial-specific p63 and cytokeratin 5/8 antibodies (Fig. 3*B*).

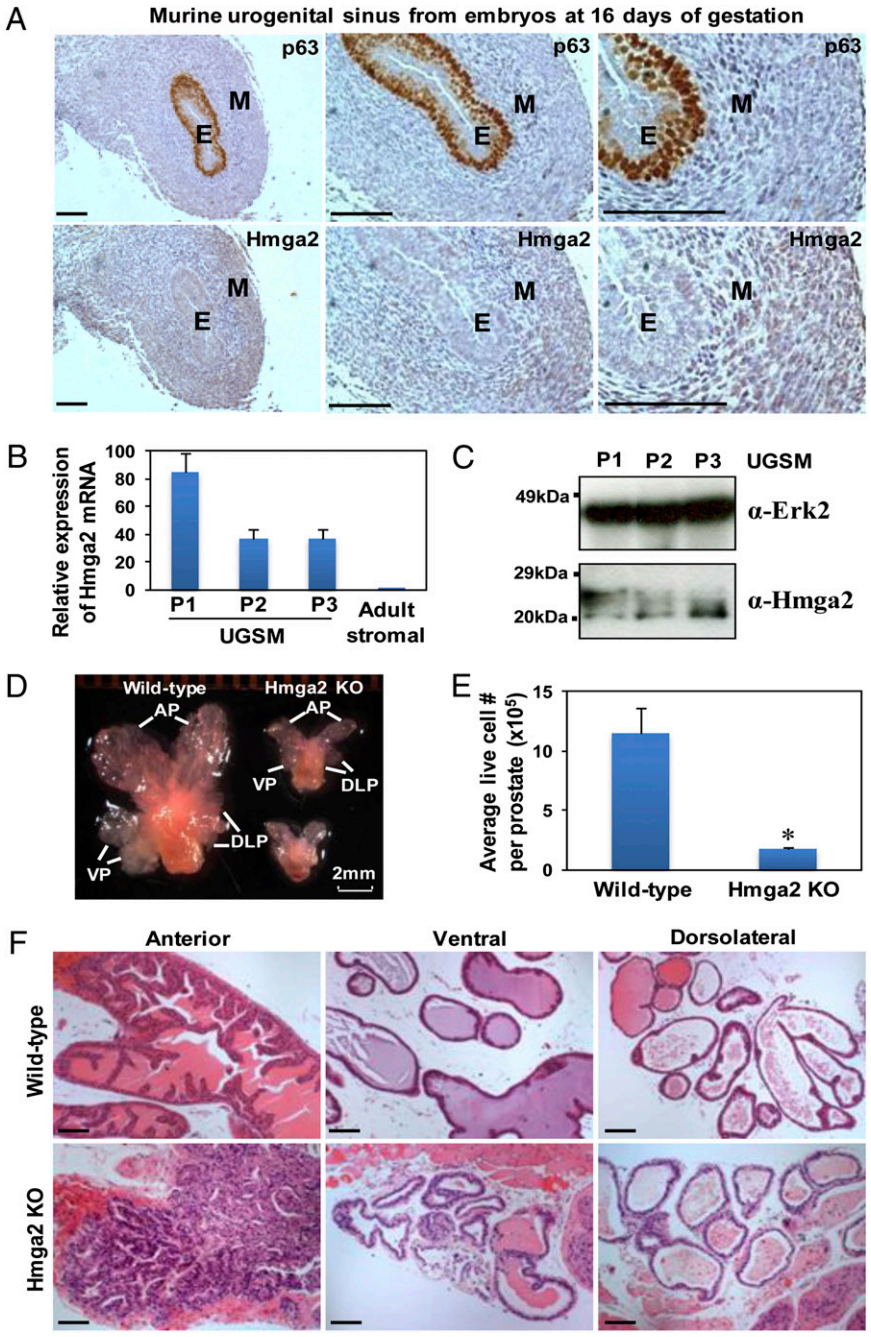

Fig. 1. Temporospatial expression of Hmga2 in murine developing UGS mesenchyme. (*A*) IHC analysis of E16 murine UGS with p63 and Hmga2 antibodies. E, epithelia; M, mesenchyme. (Scale bars, 100 μm.) (*B*) Relative expression of Hmga2 mRNA in cultured UGSM cells with different passage determined by quantitative PCR, with comparison with that in FACS-sorted adult prostate stromal (Lin-CD49f-Sca-1$^+$) cells. Data are presented as mean ± SD after normalization with Gapdh expression. (*C*) Immunoblotting of UGSM cells with anti-Hmga2 and Erk2 as a loading control. (*D*) Representative photograph of prostate glands from 11-wk-old wild-type and *Hmga2* knockout (KO) mice. AP, anterior prostate; VP, ventral prostate; DLP, dorsolateral prostate. (*E*) Comparison of live cells in dissociated prostate glands from wild-type and *Hmga2* KO mice, determined by trypan blue exclusion and represented as mean ± SD. *$P < 0.05$. (*F*) Histological analysis of different lobes of prostate from *Hmga2* KO mice and the aged-matched normal control. H&E staining. (Scale bars, 100 μm.)

Androgen depletion achieved by surgical castration after 2 mo of engraftment significantly lowered the tumor burden, evidenced by the descending growth curve, smaller size, and decreased weight of Hmga2-UGSM grafts from castrated recipients (Fig. S3 *A*–*C*). Histological and IHC analysis of grafts from castrated mice revealed an apparent shrinkage of preneoplastic glands with reduced lumens, condensed cytoplasm, loss of AR nuclear staining, and an enrichment for p63$^+$ basal cells (Fig. S3*D*), indicating that Hmga2-UGSM–induced PIN remains sensitive to androgen ablation.

Prostate Basal Stem Cells Preferentially Respond to the Growth-Promoting Effects of Hmga2-UGSM Cells. Prostate epithelia are mainly composed of three differentiated cell types: basal, luminal, and neuroendocrine cells. Our previous studies demonstrated that murine prostate stem cells can be enriched using cell surface markers, namely Lin-Sca-1$^+$CD49f$^+$ (LSC). This subpopulation of prostate epithelial cells exhibits the basal lineage traits and is susceptible to malignant transformation induced by multiple oncogenic events (29). To identify prostate epithelial

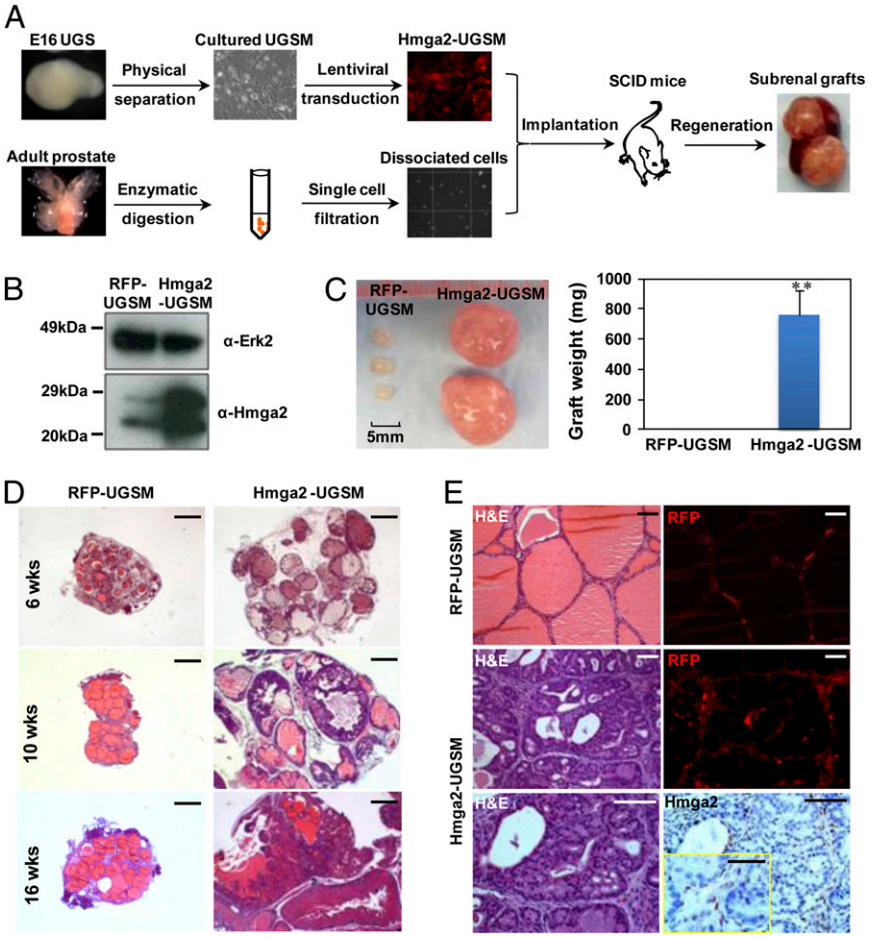

Fig. 2. Overexpression of Hmga2 in the stroma leads to the formation of multifocal high-grade PIN lesions. (*A*) Schematic design for the dissociated prostate regeneration assay. Dissociated prostate cells from wild-type adult mice were combined with lentiviral-transduced UGSM cells that were originally derived from E16 mouse UGS mesenchyme and engrafted into the subrenal capsules of male immunodeficient mice for in vivo regeneration. (*B*) Western blotting of *Hmga2*-transduced UGSM cells. (*C*) Representative prostate grafts derived from wild-type adult murine prostate cells and Hmga2-UGSM cells, compared with control grafts. Data are presented as mean ± SD. $^{**}P < 0.01$. (*D*) Histological sections of prostate regenerated tissues harvested at the indicated time points after engraftment. H&E staining. (Scale bars, 1 mm.) (*E*) Hmga2 staining with corresponding H&E and fluorescent (RFP) images of prostate regenerated tissue sections. (Scale bars, 100 μm for main images, 50 μm for *Inset*.)

cells that respond to the growth-promoting effects of Hmga2-modified stroma, we isolated LSC cells and luminal (Lin-Sca-1-CD49f^{low}) epithelial cells from normal adult murine prostate tissue and directly compared the responses of these two cell lineages to the effects of Hmga2-UGSM cells. After 8–12 wk of regeneration, the grafts derived from LSC cells displayed a significant premalignant phenotype, evidenced by increased graft size and weight, extensive epithelial tufting, and gland enlargement (Fig. 3 *C* and *D*). In contrast, small tissue recombinants consisting of luminal cells and Hmga2-UGSM cells were harvested from the recipient mice. Very rare tubule formation with mild epithelial stratification was observed in those grafts derived from luminal cells. These data further support that the observed PIN lesions are of adult prostate epithelial origin and indicate that an enriched subpopulation of prostate stem-like basal cells preferentially respond to the growth-promoting effects of Hmga2-modified stroma.

Sustained Overexpression of Hmga2 in Stromal Cells Is Required for Tumor Maintenance. Mounting evidence suggests that some cancers are dependent on essential genes for tumor maintenance; however, certain tumors acquire oncogene independence due to secondary mutations (34). To test whether continuous expression of Hmga2 in the stroma is required for PIN maintenance, a doxycycline (DOX)-inducible *Hmga2* lentiviral vector (TRE-*Hmga2*) was constructed, and UGSM cells expressing rtTA protein were prepared from R26-M2rtTA transgenic mice. The in vivo regeneration assay was performed using dissociated adult prostate cells from wild-type mice, and systemic administration of DOX was started on day 1 after engraftment (Fig. 4*A*). After 8 wk of regeneration and DOX induction, multifocal PIN lesions were developed (Fig. 4*B*), whereas no abnormality was observed in the control grafts from DOX-untreated recipients. Hmga2 expression was readily detected in the fibromuscular layer surrounding PIN lesions in DOX-treated grafts but was undetectable in uninduced grafts (Fig. 4*D*). The severity of the preneoplastic phenotype was closely associated with Hmga2 levels regulated by DOX dosage (Fig. 4 *B* and *C*), suggesting tight regulation in this inducible system. Importantly, DOX withdrawal after the 8-wk induction led to notable regression of PIN lesions, evidenced by reduction of graft weight, loss of complex glandular architecture, and decreased burden of precancerous cells replaced largely by simple glands with abundant secretions (Fig. 4 *E* and *F*). These results indicate that sustained overexpression of stromal Hmga2 is required for tumor maintenance.

Wnt Ligands Are the Major Paracrine Mediators for the Growth-Promoting Effects of Hmga2-Modified Stroma. Epithelial and microenvironmental interactions can be accomplished by juxtacrine,

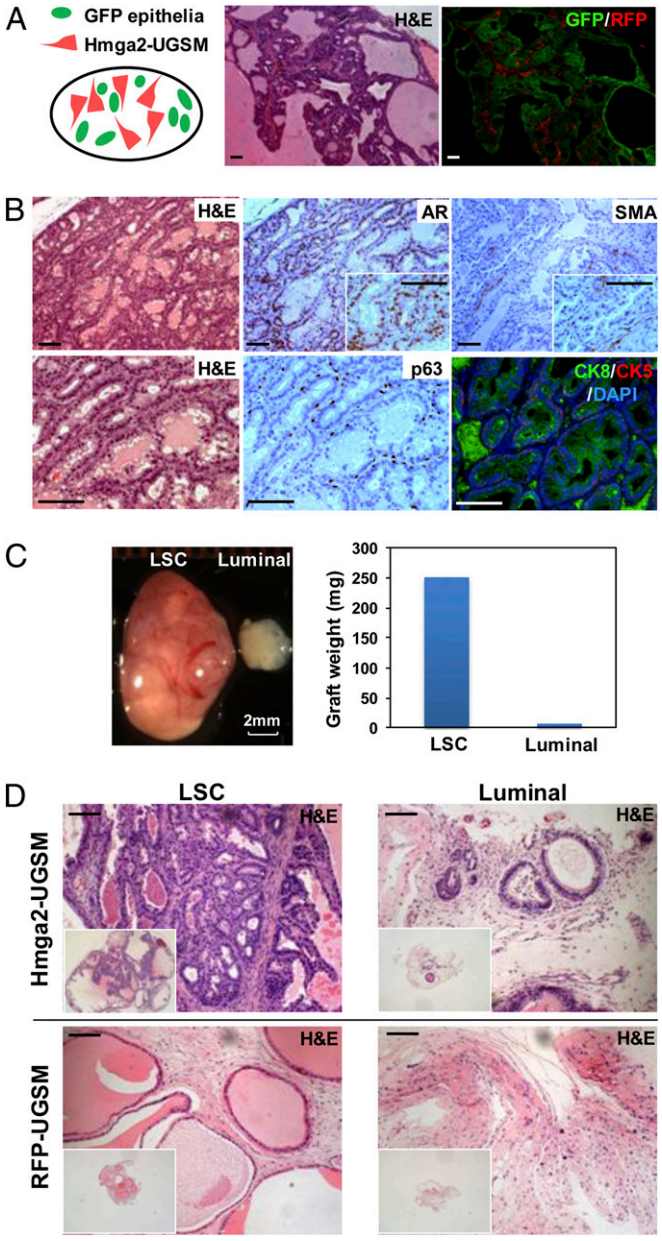

Fig. 3. Hmga2-UGSM cells induced PIN lesions are of adult prostate epithelial origin, and prostate basal stem cells preferentially respond to the growth-promoting effects of Hmga2-modified stroma. (*A*) Representative histological section and corresponding fluorescent photo of prostate grafts derived from Hmga2-UGSM cells and adult prostate cells from GFP transgenic mice. (*B*) IHC analysis of Hmga2-UGSM grafts with the indicated antibodies. (Scale bars, 100 μm.) (*C*) Representative photograph and weight measurement of Hmga2-UGSM grafts derived from prostate stem cells-enriched (LSC) basal cells or luminal epithelial cells. (*D*) H&E staining of Hmga2-UGSM grafts and RFP-UGSM grafts derived from LSC (basal-enriched) cells or luminal epithelial cells. (Scale bars, 100 μm.)

paracrine, or endocrine mechanisms. Tissue recombinants containing RFP-UGSM cells were implanted together with grafts containing Hmga2-UGSM cells into the same kidney capsule (Fig. S4*A*). The grafts derived from RFP-UGSM cells did not exhibit any abnormality when they were grown in immediate proximity to Hmga2 grafts (Fig. S4*B*), suggesting that Hmga2-modified stromal cells induce PIN via localized mechanisms. To explore the downstream mediators responsible for the growth-promoting effects of Hmga2-UGSM cells, we performed microarray analysis to compare the global gene profiles that were differentially expressed between Hmga2-UGSM cells and control cells. Surprisingly, only a small number of genes were identified to be up-regulated or down-regulated more than twofold after Hmga2 overexpression for 4–6 d (Fig. 5*A* and Fig. S5 *A* and *B*). Previous work showed that Hmga2 overexpression displaces histone deacetylase (HDAC) from chromatin and causes increased acetylation of histone H3 on target gene promoters (22, 35). We performed immunoblotting and immunofluorescence assays to characterize the epigenetic changes induced by Hmga2 overexpression and found a notable increase in histone acetylation at H3 lysine 9/14 in Hmga2-UGSM cells (Fig. S5 *C* and *D*).

Antibody staining was used to survey the pathways activated in premalignant lesions to identify the potential localized factors responsible for the growth-promoting effects of Hmga2-modified stroma. In contrast to negative or weak staining of phospho-Akt, phospho-S6K, phospho-Erk, phospho-Jak2, phospho-Stat3, and phospho-Stat5, significant β-catenin accumulation was detected in preneoplastic epithelia in prostate grafts with stromal overexpression of Hmga2 (Fig. 5*B*). Although strong nuclear β-catenin staining was only observed in a fraction of epithelial cells, increased levels of cytoplasmic and membrane-associated β-catenin were evident. Consistently, c-Myc, a known target gene of β-catenin (36), was up-regulated in Hmga2-UGSM grafts (Fig. 5*C*).

Adult prostate cells from β-catenin conditional knockout mice were transduced with a *Cre*/*GFP* lentivirus, and the regeneration assay was performed to determine whether epithelial β-catenin is required for Hmga2-UGSM–induced PIN. We found that in contrast to the adjacent preneoplastic glands derived from nontransduced epithelial cells, Cre-mediated deletion of β-catenin in prostate epithelia significantly inhibited the development of PIN lesions induced by Hmga2-UGSM (Fig. 5*D*). This suggests that epithelial β-catenin participates in tumorigenesis induced by Hmga2-modified stroma. Given the central role of β-catenin in the canonical Wnt pathway and the short-range cell–cell signaling of Wnt ligands due to their tight association with the ECM and the cell surface (37), we hypothesized that Wnt ligands are the potential paracrine mediators for the growth-promoting effects of Hmga2-UGSM cells. Quantitative PCR analysis of 19 Wnt ligands revealed that the expression of Wnt2, Wnt4, and Wnt9a were increased more than fivefold in Hmga2-UGSM cells compared with those in RFP-UGSM cells (Fig. 5*E*). Treatment of UGSM cells with an HDAC inhibitor, trichostatin A, significantly up-regulated Wnt2 and Wnt4 mRNA expression (Fig. S5*E*), which mimics the effects of Hmga2 overexpression in UGSM cells. It indicates that the Hmga2-mediated increase in H3K9/K14 acetylation may be associated with elevated Wnt expression in Hmga2-UGSM cells.

Overexpression of Wnt Antagonists in the Stroma Strongly Suppresses Hmga2-UGSM–Induced PIN. To confirm that the growth-promoting effects of Hmga2-UGSM cells are mediated by augmented Wnt signaling, lentiviral vectors were constructed to overexpress specific Wnt antagonists, Dickkopf-related protein 1 (Dkk1) or secreted frizzled-related protein 2 (Sfrp2). These two secreted proteins inhibit Wnt signaling via binding to the LRP5/6 coreceptor or interacting with secreted Wnt ligands and Frizzled receptors, respectively (Fig. 6*A* and Fig. S6*A*) (38). Coexpression of either Dkk1 or Sfrp2 with Hmga2 in UGSM cells partially inhibited the development of PIN, evidenced by a 1.8- to 2.5-fold reduction of graft weight, attenuated epithelial stratification, and smaller lumens (Fig. 6 *B*–*E*). When a combination of Dkk1 and Sfrp2 was overexpressed in Hmga2-UGSM cells, there was a remarkable decrease in graft size and weight (approximately eightfold) relative to Hmga2-UGSM grafts (Fig. 6*F*). In sharp contrast to high-grade PIN in Hmga2-UGSM grafts, only a few glands with modest epithelial tufting were observed in grafts derived from UGSM cells coexpressing Hmga2, Dkk1, and Sfrp2

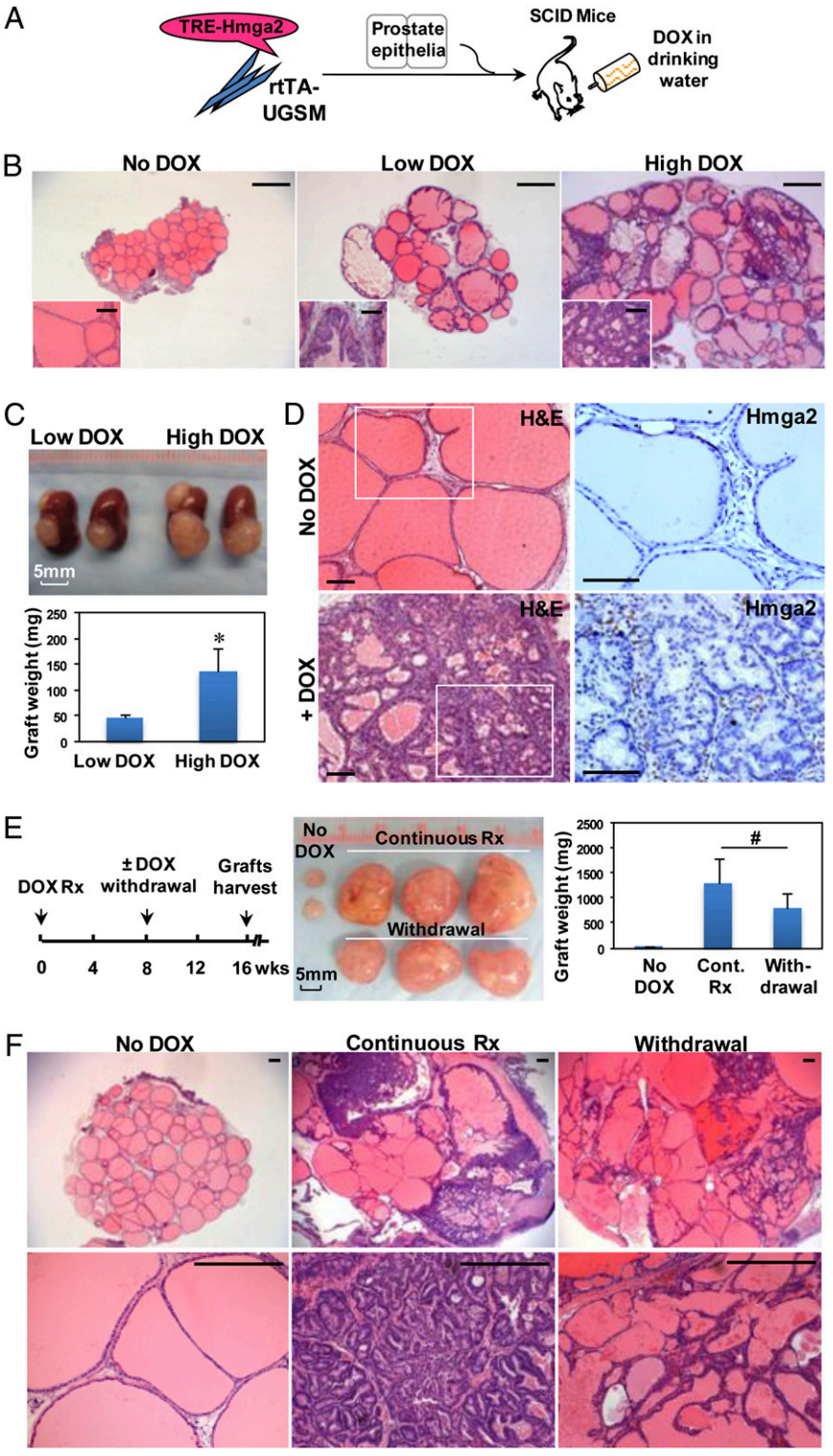

Fig. 4. Devolvement and maintenance of PIN lesions are dependent on continuous expression of Hmga2 in the stroma. (*A*) Diagram of the approach used to assess the requirement of stromal Hmga2 for the maintenance of PIN lesions. The rtTA-expressing UGSM cells were infected with DOX-inducible *Hmga2* lentivirus (TRE-*Hmga2*). The in vivo regeneration assay was performed using dissociated adult normal prostate cells in the absence or presence of systemic administration of DOX. TRE, tetracycline responsive element; rtTA, reverse tetracycline-controlled transactivator. (*B*) Histology of prostate grafts with inducible expression of stromal Hmga2 from recipient mice treated for 8 wk with two concentrations of DOX (Low DOX: 0.4 mg/mL; High DOX: 2 mg/mL). H&E staining. (Scale bars, 1 mm for main images, 100 μm for *Insets*.) (*C*) Photograph and weight measurement of representative subrenal grafts from recipient mice treated with two concentrations of DOX. Data are presented as mean ± SD. $^{*}P < 0.05$. (*D*) Hmga2 staining of prostate regenerated tissues from DOX-uninduced mice or mice treated with 2 mg/mL DOX for 8 wk. (Scale bars, 100 μm.) (*E* and *F*) Gross appearance, graft weight, and H&E staining of prostate regenerated tissues from recipients in various treatment conditions as indicated. Data are presented as mean ± SD. $^{\#}P > 0.05$. (Scale bars, 300 μm.)

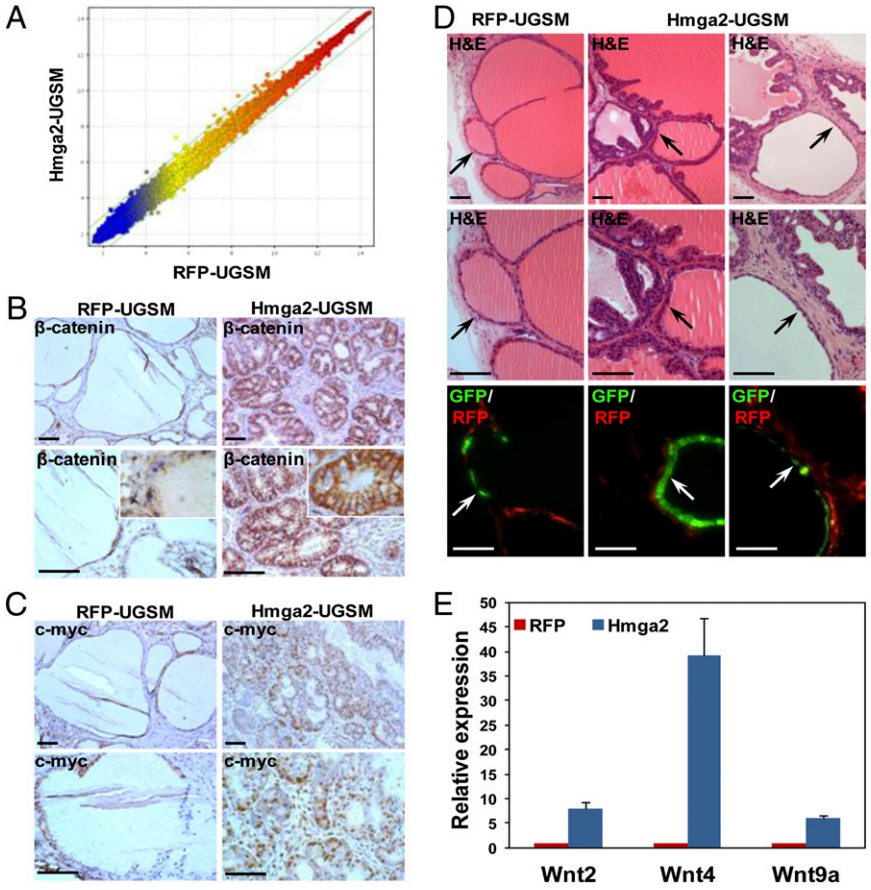

Fig. 5. Augmented Wnt/β-catenin signaling in murine PIN lesions induced by Hmga2-modified stromal cells. (*A*) Scatter plot for expression ratios of the global gene profiles between Hmga2-UGSM cells and control cells. Each dot represents the average fold change for individual genes summarized from three independent microarrays. (*B* and *C*) IHC analysis of prostate grafts with β-catenin and c-Myc antibodies. (Scale bars, 100 μm.) (*D*) Histological sections (H&E staining) and corresponding merged fluorescent images of regenerated tissues derived from *Cre*-transduced prostate cells from β-catenin$^{fl/fl}$ mice. Arrows indicate the *Cre/GFP* lentiviral transduced prostate tubules. (Scale bars, 100 μm.) (*E*) Quantitative PCR analyses of Wnt ligands differentially expressed between Hmga2-UGSM cells and RFP-UGSM control samples. Data are presented as mean ± SD after normalization with β-actin.

(Fig. 6*G*), indicating a significant synergistic effect of these Wnt antagonists. Hmga2-positive cells were easily detected in the stroma from grafts with cooverexpression of Hmga2 and Wnt inhibitors (Fig. S6*B*), and no significant decrease in tubule formation or morphological changes in prostate epithelia were observed in grafts derived from Dkk1/Sfrp2-UGSM cells (Fig. S6*E*). This indicates that the suppression of the precancerous phenotype is solely attributed to inhibition of Wnt pathway. These results strongly suggest that Wnt/β-catenin signaling is activated at the ligand/receptor level in grafts with Hmga2-modified stroma, and their growth-promoting effects are predominantly mediated by augmented paracrine Wnt/β-catenin signaling.

Cooverexpression of Hmga2 and AR in UGSM Cells Synergize to Induce Poorly Differentiated Prostate Adenocarcinoma. We monitored some recipient mice with Hmga2-UGSM grafts for ∼16 wk after engraftment, and no significant clinical signs of local invasion or distant metastasis were observed. These results are consistent with previous findings about the development of breast adenocarcinoma in Wnt-1 transgenic mice (39), suggesting that increased Wnt signaling is sufficient to initiate tumorigenesis but that other oncogenic events are necessary for full malignant transformation.

Prostate organogenesis is dependent on AR signaling in mesenchymal cells, which leads to the production of soluble factors, ECM components, and cell adhesion molecules, collectively referred to as "andromedins" (40). To test whether the paracrine effects of Hmga2-modified stroma cooperate with the andromedins, Hmga2-UGSM cells were transduced with an *AR/GFP* lentivirus and implanted in the prostate regeneration assay. This combination drove the progression of PIN lesions to poorly differentiated prostate adenocarcinoma (Fig. 7*A*). Although AR overexpression causes moderate increase in Wnt2, Wnt4 mRNA expression, and modest down-regulation of Wnt5b, Wnt10b, and Wnt16, assessed by quantitative PCR, overexpression of AR in UGSM cells alone is not sufficient to induce any hyperplastic abnormalities (Fig. 7*A* and Fig. S7). The cancer phenotype in Hmga2/AR-UGSM grafts was characterized by multiple foci of solid sheets of cytologically malignant cells, with loss of secretions and penetration of tightly packed prostate glands into the stroma (Fig. 7 *A* and *B*). Fluorescent imaging and IHC staining confirmed that prostate cancer was derived from wild-type prostate epithelial cells, which were adjacent to Hmga2/AR double-positive stromal cells (Fig. 7*C*). IHC analysis of Hmga2/AR-UGSM grafts with a pan β-catenin antibody revealed that increased accumulation of cytoplasmic and membrane-associated β-catenin was only observed in neoplastic epithelial cells in close proximity to Hmga2/AR-overexpressing stromal cells. Using an anti-active-β-catenin antibody (41), strong nuclear staining of β-catenin was scattered in the entire compartment of neoplastic epithelia (Fig. 7*C*). These results demonstrate that the growth-promoting effects of Hmga2-modifed stroma can

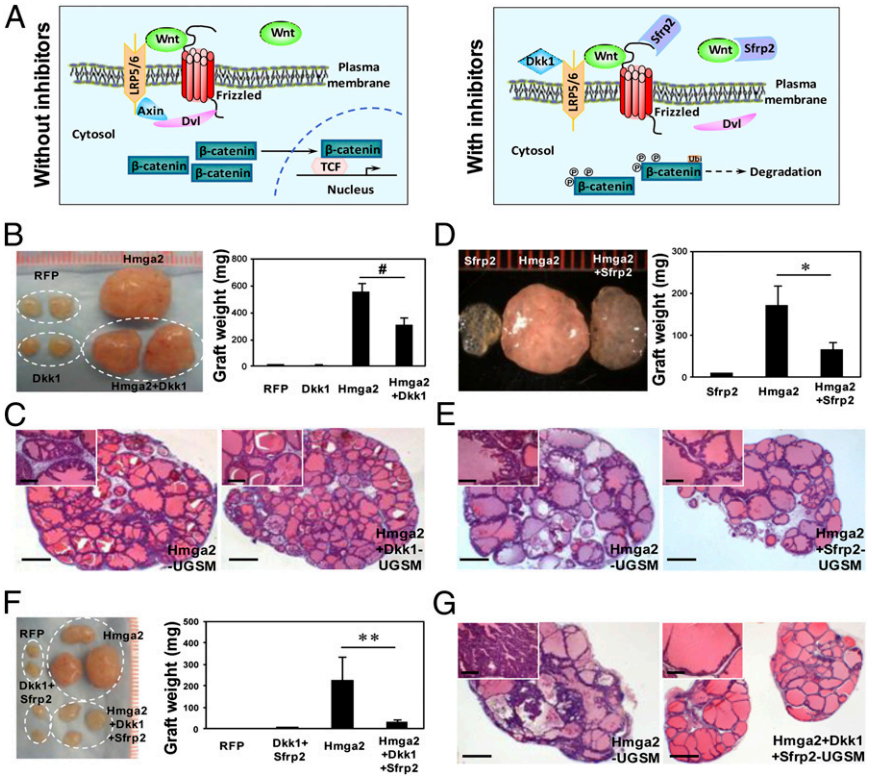

Fig. 6. Forced expression of two Wnt inhibitors in the stroma significantly suppresses Hmga2-UGSM induced PIN lesions. (*A*) Schematic representation of Wnt signaling pathway in the absence or presence of Dkk1 and Sfrp2. (*B* and *C*) Gross appearance, weight, and H&E staining of prostate grafts with stromal overexpression of Dkk1 and Hmga2. Data are presented as mean ± SD. $^{\#}P > 0.05$. (*D* and *E*) Representative photograph and histological sections of regenerated tissues derived from Hmga2 or Hmga2+Sfrp2-UGSM cells. Data are presented as mean ± SD. $^{*}P < 0.05$. (*F* and *G*) Macroscopic overview, weight, and H&E staining of prostate grafts with stromal co-overexpression of Dkk1, Sfrp2, and Hmga2. Data are expressed as mean ± SD. $^{**}P < 0.01$. (Scale bars, 1 mm for main images, 200 μm for *Insets*.)

strongly synergize with stromal AR-regulated paracrine signaling to promote prostate cancer progression.

Discussion

Increasing evidence implicates both genetic changes and epigenetic abnormalities as contributing to carcinogenesis. The potent growth-promoting effects of Hmga2-modified stroma resulted in rapid formation of multifocal high-grade PIN, indicating that carcinoma can be solely initiated by epigenetic alterations in the stroma, preceding any mutations in adjacent epithelial cells. Interestingly, it has been recently shown that HDAC inhibitor-induced chromatin remodeling in fibroblasts can promote tumor growth in a paracrine fashion (42). All these findings underscore the importance of epigenetic changes in the establishment of an aberrant tumor microenvironment for cancer initiation and progression.

High levels of HMGA2 were observed in several mesenchymal tumors and various human carcinomas (20). Although ectopic HMGA2 expression is mainly detected in the epithelia in most cancers, *HMGA2*-associated chromosomal rearrangements were found predominantly in the stromal component of mass-forming endometriosis (43), endometrial polyps, and pulmonary chondroid hamartoma that consist of both hyperplastic stromal and epithelial cells (44). We observed the stromal-specific HMGA2 overexpression by IHC analysis in several human biphasic tumors of the prostate, including phyllodes tumors of the prostate and stromal tumors of uncertain malignant potential (Fig. S8). Although these types of prostate tumor are rare in clinical practice, a large percentage of these tumors display hyperplastic changes in the epithelial compartment, which may result from aberrant mesenchymal–epithelial interactions (45, 46).

Previous studies of transgenic mice with adipocyte-specific HMGA2 expression showed that HMGA2 overexpression in the mesenchyme not only leads to the overgrowth of stromal cells but also causes epithelial hyperplasia and tumor formation in breast, uterus, salivary glands, and preputial glands (47). It seems that most tissues predisposed to the growth-promoting effects of Hmga2-modified stroma are sex hormone-regulated peripheral tissues. Although these effects could be due to tissue-specific expression of Hmga2, the mostly likely explanation is that sex hormones synergize with the paracrine effects of Hmga2-expressing stroma to drive transformation of epithelial cells. This hypothesis is supported by our findings of strong synergistic effects of combined Hmga2 and AR overexpression in UGSM cells.

Hmga2 overexpression in UGSM cells led to increased histone acetylation and enhanced production of several Wnt ligands, including Wnt4, indicating that Hmga2-mediated chromatin modification may serve as an epigenetic mechanism to regulate the Wnt signaling pathway in the stroma. It has been recently reported that Wt1-mediated chromatin remodeling regulates Wnt4 expression dichotomously in kidney mesenchyme and the epicardium (48). In addition, previous studies have shown that Wnt4 expression is controlled by histone acetylation levels in the Wnt4 promoter (49, 50). Although we cannot rule out the possibility that Hmga2 might regulate Wnt expression in a manner other than functioning as an epigenetic regulator, it seems very likely that the Hmga2-mediated increase in H3K9/K14 acetylation contributes, at least partially, to up-regulation of Wnt ligands in Hmga2-modified stroma.

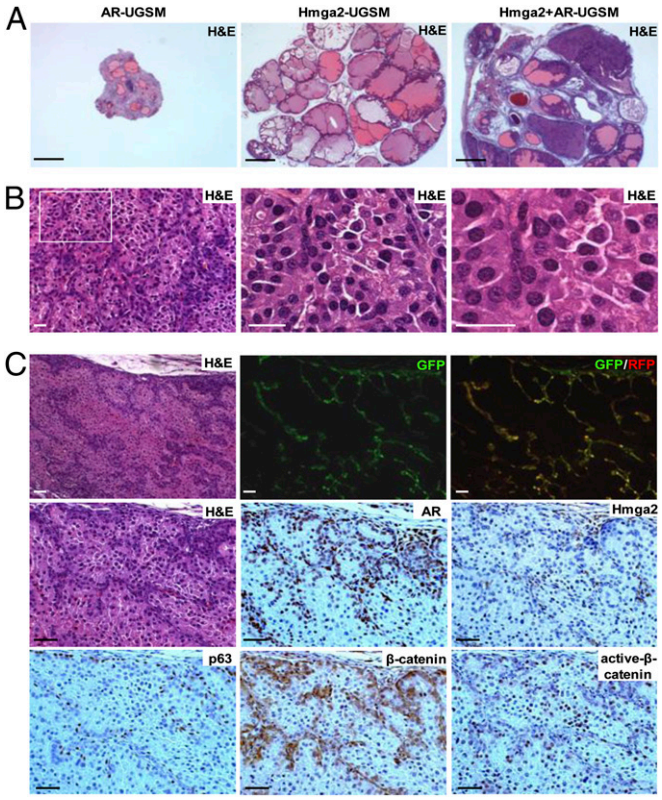

Fig. 7. Combined expression of Hmga2 and AR in the stroma results in the development of invasive prostate cancer. (*A*) Representative histological sections of prostate grafts with stromal coexpression of Hmga2 and AR. (Scale bars, 1 mm.) (*B*) H&E staining of tissue recombinants consisting of Hmga2+AR-UGSM and wild-type prostate cells. (Scale bars, 25 μm.) (*C*) IHC analysis of prostate grafts derived from Hmga2+AR-UGSM cells with various antibodies as indicated, with corresponding H&E staining and fluorescent images. (Scale bars, 50 μm.)

Our data show that pronounced β-catenin accumulation is associated with Hmga2-UGSM–induced PIN, which can be strongly suppressed by co-overexpression of Dkk1 and Sfrp2. Wnt ligands are the likely paracrine mediators for the growth-promoting effects of Hmga2-modified stroma. The Wnt pathway has been implicated in tumorigenesis of various tissue origins (38). Abnormal expression patterns of β-catenin have been observed in 20–71% of prostate cancer samples (51–53), and high levels of β-catenin are concomitantly associated with increasing Gleason score and castration resistance (53, 54). Although recent studies showed that mutations in allophycocyanin and β-catenin can be detected in approximately 10% and 12% of castration-resistant prostate cancer, respectively (55–57), it seems that Wnt/β-catenin signaling could play a more common role in prostate cancer than would be predicted by the point mutation rates of these downstream effectors (53, 58, 59). Alterations in Wnt ligands and their modulators that are secreted from prostate epithelia and the surrounding stroma may serve as the alternative mechanism for activation of Wnt signaling in a subset of human prostate cancer. Small-molecule inhibitors or specific antibodies that suppress the Wnt signaling pathway (38) may represent a novel strategy for targeted therapies in prostate cancer, especially with the successful development of the orally bioavailable porcupine inhibitors that block porcupine-dependent lipidation of Wnt proteins (60). Given the highly activated Wnt/β-catenin signaling in murine PIN lesions induced by Hmga2-modifed stroma, our model provides a useful preclinical system to screen the candidate therapeutic compounds and test the in vivo efficacies of these targeted therapies against Wnt/β-catenin signaling.

In addition, our laboratory recently demonstrates that β-catenin binds to the intracellular domain of Trop-2 and that nuclear β-catenin colocalizes with the intracellular domain of Trop-2 in human prostate cancer. Overexpression of Trop2 leads to up-regulation of the β-catenin downstream target genes cyclin D1 and c-myc, and loss of β-catenin abolishes Trop2-driven self-renewal and transformation activity (61). These findings suggest that β-catenin signaling can be activated by multiple upstream events and play an important role in prostate cancer.

Materials and Methods

Construction of Lentiviral Vectors. Details of lentiviral constructs subcloning are described in *SI Materials and Methods*. Lentiviral stocks were prepared using the calcium phosphate precipitation technique (24).

Cell Culture and Immunoblotting. Murine UGSM cells were prepared as described previously (24) and transduced with lentiviruses in the presence of 8 μg/mL polybrene. Whole-cell protein lysates (10–15 μg) were separated by SDS/PAGE followed by immunoblotting analysis using anti-Hmga2 (Abcam) and anti-ERK2 (Santa Cruz Biotechnology) antibodies.

Mice. R26-M2rtTA mice (62) and transgenic mice with chicken β-actin promoter-driven eGFP expression (63) were originally obtained from Jackson Laboratories, back-crossed to achieve the C57BL/6 background, and raised in our animal research center. Homozygous mice with floxed alleles of β-catenin (64) were purchased from Jackson Laboratories. All procedures conducted in this study were approved by the Division of Laboratory Animal Medicine of the University of California, Los Angeles.

Dissociated Prostate Regeneration Assay and DOX Treatment of Animals. In vivo prostate regeneration assays were performed as described previously (24). Prostate recombinants were implanted into the subrenal capsules of male SCID mice or s.c. as indicated, in the presence of supplemental androgen (s.c. testosterone pellets, 12.5 mg per pellet, one pellet per mouse). The grafts were dissected from the host mice 6–16 wk after engraftment, fixed, and sectioned for H&E staining and immunohistological analysis. The s.c. grafts were measured by external caliper twice per week to determine the greatest longitudinal diameter (length) and the greatest transverse diameter (width). Tumor size was calculated by the ellipsoidal volume equation ($1/2 \times L \times W^2$). For DOX induction, DOX (Sigma) was added into drinking water at the indicated concentration together with 5% (wt/vol) sucrose and refreshed every 3–4 d.

IHC and Immunofluorescence Analysis. IHC and immunofluorescence analyses of tissue sections were performed according to the previous protocols (24, 29). The following primary antibodies were used: anti-Hmga2 (BioCheck), anti-β-catenin (BD Transduction Laboratories), anti-active-β-catenin and PCNA (Millipore), c-Myc and α-smooth muscle actin (Abcam), anti-p63 and AR (Santa Cruz Biotechnology), and anti-CK5 and CK8 (Covance).

Microarray and Real-Time RT-PCR. RNA was extracted using TRIzol (Invitrogen), purified with the RNeasy micro kit (QIAGEN), and hybridized on an Affymetrix Mouse Genome 430 2.0 chip. The first-strand cDNAs were synthesized by SuperScript III reverse transcriptase (Invitrogen). Real-time PCR was carried out on the StepOne system (Applied Biosystems) using Taqman universal master mix (Applied Biosystems) or MESA FAST SYBR MasterMix (Eurogentec). Mouse *Hmga2* and *Gapdh* probes and primers were from Applied Biosystems. *Wnt* mRNA expression was compared with the comparative Ct method using mouse β-actin as the endogenous control. Primer sequences are listed in Table S1.

Statistical Analyses. The statistical differences between experimental groups were compared by two-tailed unpaired Student *t* test. A *P* value of 0.05 was chosen as the limit of statistical significance.

ACKNOWLEDGMENTS. We thank the members of the O.N.W. laboratory for technical help and scientific discussions, the Translational Pathology Core for tissue embedding and sectioning, the Clinical Microarray Core and Lai Wei for microarray assay and data analysis, Margaret Goodell for the pLTRET-Luc vector, and Roger Lo for TOPFlash and FOPFlash plasmids. We are grateful to Drs. Hong Wu and Siavash Kurdistani for their helpful comments and Dr. Sanaz Memarzadeh for critical reading of the manuscript. This work was

partly supported by funds from a Prostate Cancer Foundation challenge award and National Cancer Institute Grant 1U01CA164188. O.N.W. is an Investigator and Y.Z. is an Associate of the Howard Hughes Medical Institute. J.H. is also supported by US Department of Defense Prostate Cancer Research Program Grant PC1001008, University of California, Los Angeles Specialized Program of Research Excellence in prostate cancer [Principal Investigator (PI), R. Reiter], a creativity award from the Prostate Cancer Foundation (PI, M. Rettig), and National Institutes of Health Grant 1R01CA158627 (PI, L. Marks).

1. Siegel R, Naishadham D, Jemal A (2012) Cancer statistics, 2012. *CA Cancer J Clin* 62(1): 10–29.
2. Andreoiu M, Cheng L (2010) Multifocal prostate cancer: Biologic, prognostic, and therapeutic implications. *Hum Pathol* 41(6):781–793.
3. Slaughter DP, Southwick HW, Smejkal W (1953) Field cancerization in oral stratified squamous epithelium; clinical implications of multicentric origin. *Cancer* 6(5):963–968.
4. Bhowmick NA, et al. (2004) TGF-beta signaling in fibroblasts modulates the oncogenic potential of adjacent epithelia. *Science* 303(5659):848–851.
5. Memarzadeh S, et al. (2007) Enhanced paracrine FGF10 expression promotes formation of multifocal prostate adenocarcinoma and an increase in epithelial androgen receptor. *Cancer Cell* 12(6):572–585.
6. Hill R, Song Y, Cardiff RD, Van Dyke T (2005) Selective evolution of stromal mesenchyme with p53 loss in response to epithelial tumorigenesis. *Cell* 123(6):1001–1011.
7. Bissell MJ, Kenny PA, Radisky DC (2005) Microenvironmental regulators of tissue structure and function also regulate tumor induction and progression: The role of extracellular matrix and its degrading enzymes. *Cold Spring Harb Symp Quant Biol* 70: 343–356.
8. Eng C, Leone G, Orloff MS, Ostrowski MC (2009) Genomic alterations in tumor stroma. *Cancer Res* 69(17):6759–6764.
9. Allinen M, et al. (2004) Molecular characterization of the tumor microenvironment in breast cancer. *Cancer Cell* 6(1):17–32.
10. Qiu W, et al. (2008) No evidence of clonal somatic genetic alterations in cancer-associated fibroblasts from human breast and ovarian carcinomas. *Nat Genet* 40(5): 650–655.
11. Orimo A, et al. (2005) Stromal fibroblasts present in invasive human breast carcinomas promote tumor growth and angiogenesis through elevated SDF-1/CXCL12 secretion. *Cell* 121(3):335–348.
12. Hu M, et al. (2005) Distinct epigenetic changes in the stromal cells of breast cancers. *Nat Genet* 37(8):899–905.
13. Schaeffer EM, et al. (2008) Androgen-induced programs for prostate epithelial growth and invasion arise in embryogenesis and are reactivated in cancer. *Oncogene* 27(57):7180–7191.
14. Wong DJ, et al. (2008) Module map of stem cell genes guides creation of epithelial cancer stem cells. *Cell Stem Cell* 2(4):333–344.
15. Ben-Porath I, et al. (2008) An embryonic stem cell-like gene expression signature in poorly differentiated aggressive human tumors. *Nat Genet* 40(5):499–507.
16. Takahashi K, Yamanaka S (2006) Induction of pluripotent stem cells from mouse embryonic and adult fibroblast cultures by defined factors. *Cell* 126(4):663–676.
17. Yu J, et al. (2007) Induced pluripotent stem cell lines derived from human somatic cells. *Science* 318(5858):1917–1920.
18. Hochedlinger K, Plath K (2009) Epigenetic reprogramming and induced pluripotency. *Development* 136(4):509–523.
19. Viswanathan SR, Daley GQ (2010) Lin28: A microRNA regulator with a macro role. *Cell* 140(4):445–449.
20. Fusco A, Fedele M (2007) Roles of HMGA proteins in cancer. *Nat Rev Cancer* 7(12): 899–910.
21. Nishino J, Kim I, Chada K, Morrison SJ (2008) Hmga2 promotes neural stem cell self-renewal in young but not old mice by reducing p16Ink4a and p19Arf Expression. *Cell* 135(2):227–239.
22. Fedele M, et al. (2006) HMGA2 induces pituitary tumorigenesis by enhancing E2F1 activity. *Cancer Cell* 9(6):459–471.
23. Kishi Y, Fujii Y, Hirabayashi Y, Gotoh Y (2012) HMGA regulates the global chromatin state and neurogenic potential in neocortical precursor cells. *Nat Neurosci* 15(8): 1127–1133.
24. Xin L, Ide H, Kim Y, Dubey P, Witte ON (2003) In vivo regeneration of murine prostate from dissociated cell populations of postnatal epithelia and urogenital sinus mesenchyme. *Proc Natl Acad Sci USA* 100(Suppl 1):11896–11903.
25. Zhou X, Benson KF, Ashar HR, Chada K (1995) Mutation responsible for the mouse pygmy phenotype in the developmentally regulated factor HMGI-C. *Nature* 376(6543): 771–774.
26. D'Armiento J, et al. (2007) Identification of the benign mesenchymal tumor gene HMGA2 in lymphangiomyomatosis. *Cancer Res* 67(5):1902–1909.
27. Sgarra R, et al. (2009) Macroscopic differences in HMGA oncoproteins post-translational modifications: C-terminal phosphorylation of HMGA2 affects its DNA binding properties. *J Proteome Res* 8(6):2978–2989.
28. Caron L, Bost F, Prot M, Hofman P, Binétruy B (2005) A new role for the oncogenic high-mobility group A2 transcription factor in myogenesis of embryonic stem cells. *Oncogene* 24(41):6281–6291.
29. Lawson DA, et al. (2010) Basal epithelial stem cells are efficient targets for prostate cancer initiation. *Proc Natl Acad Sci USA* 107(6):2610–2615.
30. Anand A, Chada K (2000) In vivo modulation of Hmgic reduces obesity. *Nat Genet* 24(4):377–380.
31. Ellwood-Yen K, et al. (2003) Myc-driven murine prostate cancer shares molecular features with human prostate tumors. *Cancer Cell* 4(3):223–238.
32. Wang S, et al. (2003) Prostate-specific deletion of the murine Pten tumor suppressor gene leads to metastatic prostate cancer. *Cancer Cell* 4(3):209–221.
33. Zong Y, et al. (2009) ETS family transcription factors collaborate with alternative signaling pathways to induce carcinoma from adult murine prostate cells. *Proc Natl Acad Sci USA* 106(30):12465–12470.
34. Weinstein IB, Joe AK (2006) Mechanisms of disease: Oncogene addiction—a rationale for molecular targeting in cancer therapy. *Nat Clin Pract Oncol* 3(8):448–457.
35. Li AY, et al. (2011) High-mobility group A2 protein modulates hTERT transcription to promote tumorigenesis. *Mol Cell Biol* 31(13):2605–2617.
36. He TC, et al. (1998) Identification of c-MYC as a target of the APC pathway. *Science* 281(5382):1509–1512.
37. Cadigan KM, Nusse R (1997) Wnt signaling: A common theme in animal development. *Genes Dev* 11(24):3286–3305.
38. Clevers H, Nusse R (2012) Wnt/β-catenin signaling and disease. *Cell* 149(6):1192–1205.
39. Tsukamoto AS, Grosschedl R, Guzman RC, Parslow T, Varmus HE (1988) Expression of the int-1 gene in transgenic mice is associated with mammary gland hyperplasia and adenocarcinomas in male and female mice. *Cell* 55(4):619–625.
40. Thomson AA (2008) Mesenchymal mechanisms in prostate organogenesis. *Differentiation* 76(6):587–598.
41. van Noort M, Meeldijk J, van der Zee R, Destree O, Clevers H (2002) Wnt signaling controls the phosphorylation status of beta-catenin. *J Biol Chem* 277(20):17901–17905.
42. Pazolli E, et al. (2012) Chromatin remodeling underlies the senescence-associated secretory phenotype of tumor stromal fibroblasts that supports cancer progression. *Cancer Res* 72(9):2251–2261.
43. Medeiros F, et al. (2010) HMGA1 and HMGA2 rearrangements in mass-forming endometriosis. *Genes Chromosomes Cancer* 49(7):630–634.
44. Tallini G, et al. (2000) HMGI-C and HMGI(Y) immunoreactivity correlates with cytogenetic abnormalities in lipomas, pulmonary chondroid hamartomas, endometrial polyps, and uterine leiomyomas and is compatible with rearrangement of the HMGI-C and HMGI(Y) genes. *Lab Invest* 80(3):359–369.
45. Morikawa T, et al. (2006) Phyllodes tumor of the prostate with exuberant glandular hyperplasia. *Pathol Int* 56(3):158–161.
46. Nagar M, Epstein JI (2011) Epithelial proliferations in prostatic stromal tumors of uncertain malignant potential (STUMP). *Am J Surg Pathol* 35(6):898–903.
47. Zaidi MR, Okada Y, Chada KK (2006) Misexpression of full-length HMGA2 induces benign mesenchymal tumors in mice. *Cancer Res* 66(15):7453–7459.
48. Essafi A, et al. (2011) A wt1-controlled chromatin switching mechanism underpins tissue-specific wnt4 activation and repression. *Dev Cell* 21(3):559–574.
49. Devgan V, Mammucari C, Millar SE, Brisken C, Dotto GP (2005) p21WAF1/Cip1 is a negative transcriptional regulator of Wnt4 expression downstream of Notch1 activation. *Genes Dev* 19(12):1485–1495.
50. Zhang H, Singh RR, Talukder AH, Kumar R (2006) Metastatic tumor antigen 3 is a direct corepressor of the Wnt4 pathway. *Genes Dev* 20(21):2943–2948.
51. Wan X, et al. (2012) Activation of β-catenin signaling in androgen receptor-negative prostate cancer cells. *Clin Cancer Res* 18(3):726–736.
52. Yardy GW, et al. (2009) Mutations in the AXIN1 gene in advanced prostate cancer. *Eur Urol* 56(3):486–494.
53. Yardy GW, Brewster SF (2005) Wnt signalling and prostate cancer. *Prostate Cancer Prostatic Dis* 8(2):119–126.
54. de la Taille A, et al. (2003) Beta-catenin-related anomalies in apoptosis-resistant and hormone-refractory prostate cancer cells. *Clin Cancer Res* 9(5):1801–1807.
55. Grasso CS, et al. (2012) The mutational landscape of lethal castration-resistant prostate cancer. *Nature* 487(7406):239–243.
56. Barbieri CE, et al. (2012) Exome sequencing identifies recurrent SPOP, FOXA1 and MED12 mutations in prostate cancer. *Nat Genet* 44(6):685–689.
57. Beltran H, et al. (2012) Targeted next-generation sequencing of advanced prostate cancer identifies potential therapeutic targets and disease heterogeneity. *Eur Urol*, 10.1016/j.eururo.2012.08.053.
58. Kypta RM, Waxman J (2012) Wnt/beta-catenin signalling in prostate cancer. *Nat Rev Urol*, 10.1038/nrurol.2012.116.
59. Sun Y, et al. (2012) Treatment-induced damage to the tumor microenvironment promotes prostate cancer therapy resistance through WNT16B. *Nat Med*, 10.1038/nm.2890.
60. Lum L, Clevers H (2012) Cell biology. The unusual case of Porcupine. *Science* 337(6097): 922–923.
61. Stoyanova T, et al. (2012) Regulated proteolysis of Trop2 drives epithelial hyperplasia and stem cell self-renewal via β-catenin signaling. *Genes Dev* 26(20):2271–2285.
62. Hochedlinger K, Yamada Y, Beard C, Jaenisch R (2005) Ectopic expression of Oct-4 blocks progenitor-cell differentiation and causes dysplasia in epithelial tissues. *Cell* 121(3):465–477.
63. Okabe M, Ikawa M, Kominami K, Nakanishi T, Nishimune Y (1997) 'Green mice' as a source of ubiquitous green cells. *FEBS Lett* 407(3):313–319.
64. Brault V, et al. (2001) Inactivation of the beta-catenin gene by Wnt1-Cre-mediated deletion results in dramatic brain malformation and failure of craniofacial development. *Development* 128(8):1253–1264.